ORIGINAL ARTICLE

Enhanced bioconversion of grass straw into bioethanol by a novel consortium of lignocellulolytic bacteria aided by combined alkaline-acid pretreatment

Priyadarshani S. Sadalage[1] · Mudasir A. Dar[2] · Ana Cláudia Paiva-Santos[3,4] · Kiran D. Pawar[1]

Abstract

Grass straw represents an attractive and renewable resource for the production of value-added products like bioethanol. However, due to its recalcitrant structure and heterogeneity, efficient biodegradation of the grass straw remains a challenge for biorefinery. In view of this objective, the efficiency of the bacterial consortium was evaluated on grass straw pretreated with mild alkaline acid solutions. The results revealed that the pretreatment of the grass straw significantly enhanced the saccharification efficiency of the bacterial consortium. The Fourier transform infrared spectroscopy (FTIR), and X-ray diffraction (XRD) analyses revealed that chemical pretreatment altered the structure of the grass straw, removing the majority of the lignin and hydrogen bonding between cellulose and hemicellulose. The field emission scanning electron microscopy (FESEM) showed an altered surface of the pretreated grass straw with pores and tunnels. During saccharification, the highest reducing sugars (224.33 ± 1.15 µg/mL) were released for 3% grass straw loadings using 2.5% of the bacterial consortium after 14 days of incubation, signifying the synergism of bacterial strains for lignocellulose bioconversion. Subsequently, the highest ethanol yield of 3.59 ± 0.85% (v/v) was attained at pH 5.5 on the 4th day of fermentation by *Saccharomyces cerevisiae* using 8% of yeast culture/inoculum. The overall obtained results highlight the significance of the cellulolytic bacterial consortium towards lignocellulosic biorefinery by secreting grass straw hydrolyzing cellulases and hemicellulases, signifying its valorization as feedstock as well as ethanol fermentation.

Keywords Bacterial consortium · Chemical pretreatment · Biomass processing · Grass straw · Lignocellulose valorization · Biorefinery

Abbreviations

LCB	Lignocellulosic biomass
GS	Grass straw
UT	Untreated
CT	Chemically pretreated
UT-GS	Untreated Grass straw
CT-GS	Chemically pretreated Grass straw
BMS	Berg minimal salt media
CrI	Crystallinity index
SHF	Separate hydrolysis and fermentation
FTIR	Fourier transform infrared spectroscopy
EDS	Energy dispersive X-ray spectrometer
XRD	X-ray diffraction
FESEM	Field emission scanning electron microscopy

Highlights

- Structural and chemical changes were observed after mild alkali-acid pretreatment of GS.
- Biomass loading and consortia volume significantly enhance reducing sugar production.
- Bioethanol production was evaluated by optimizing the effects of various parameters.
- Optimum concentration of ethanol (3.59 ± 0.85%) was obtained at 3% of biomass loading.
- The enzymatic hydrolysis improved the ability of CT-GS to produce of bioethanol.

Extended author information available on the last page of the article

1 Introduction

As the energy demand–supply gap widens, energy shortage due to limited fossil fuel resources has become a global issue. Nowadays, feedstock-based bioethanol is a promising alternative to fossil fuels. It is a renewable energy source that can reduce environmental damage caused by fossil fuels [1]. The feedstocks used to produce bioethanol can be categorized as sucrose-based feedstocks (sugar beet, sugar cane, and fruits, etc.), starch-based feedstocks (barley,

wheat, rice, corn, and potatoes, etc.), and lignocellulosic biomass (LCB) based (wood, straw, husks, and grasses) [2, 3]. Among these renewable resources, LCB, such as grass straw (GS), offers a low-cost raw material with high availability for various industrial applications [4, 5]. The global production of straw-based lignocellulosic biomass, including GS, is approximately 7 billion tons [6] and generally consists of ~ 29–50% of cellulose, ~ 25–43% of hemicellulose, and 5–18% of lignin [7, 8] while major portion being burnt in open fields, augmenting greenhouse gas emissions [9]. A careful disposal strategy of straw lignocellulose would not only prevent secondary pollution but would also allow its utilization for the biofuel industry [10]. The GS is a renewable resource that can be utilized as an alternate and sustainable energy resource to meet the future demands of energy [11]. Within the realm of lignocellulose resources, grasses, primarily classified as monocots, or Poaceae (formerly Gramineae), attract attention for a variety of reasons. Compared to wood, the lignin content of grasses is often low, but they contain a higher amount of hydrolysable and fermentable polysaccharides. Noteworthy for their annual life cycle, grasses can serve as excellent examples of renewable resources [12]. Consequently, extensive research endeavors persistently focus on unraveling the unique structural and chemical attributes of grasses with a focus on optimizing methodologies for harnessing their considerable potential in lignocellulosic biorefinery [13, 14]. The bioconversion of GS is a suitable feedstock for biofuel production with minimum greenhouse gas emissions [15]. However, the recalcitrance of the GS impedes bioconversion into monomer sugars, thereby hindering its valorization for biorefinery. This recalcitrance is clearly attributed to its complex structure and chemical composition caused by hydrogen bonding between major components such as lignin, hemicellulose, and cellulose. Additionally, an essential factor affecting the degradability of GS is its degree of polymerization and crystallinity [16, 17]. The complex and recalcitrant nature of LCB is caused by the exceptional crystalline structure, high degree of polymerization (up to 10,000 units), and presence of a complex network of inter- and intra-molecularly hydrogen-bonded hydroxyl groups in cellulose [18]. Although hemicellulose is a heteropolymer of 5- and 6-carbon sugars, it does not significantly contribute to the recalcitrance of LCB [19]. The presence of reducing sugars in both cellulose and hemicellulose increases their industrial values as a key resource of several commercially useful chemicals [20]. In contrast, lignin is a complex and heterogeneous compound composed of methoxylated phenylpropanoid units such as sinaphyl alcohol, coniferyl alcohol, and p-coumaryl alcohol. Lignin is majorly responsible for the recalcitrance of LCB, thus impeding its industrial significance. Consequently, LCB requires a pretreatment to degrade the lignin structure and expose the cellulose and

hemicellulose polymers to enzymatic actions [21, 22]. Moreover, the removal of lignin also promotes enzyme–substrate interaction and improves saccharification efficiency as well as sugar hydrolysis [23]. A mild pretreatment of the LCB with inorganic solvents like acids and alkalis is preferred due to the high conversion rate (above 90%) of sugars and fast reactions [24]. The bioconversion of lignocellulosic GS into bioethanol is carried out through thermochemical as well as biochemical routes. However, the microorganisms mediated biodegradation offers an environment friendly, strategic and economic approach from the sustainability viewpoints. Microorganisms have evolved physiological traits to obtain energy from plant biomass, breaking down cell walls and releasing sugar monomers which can be utilized for their own metabolism and fermentation purposes [25]. Among microbes, bacteria are the most prevalent biological creatures in nature due to their ability to decompose natural polymers like cellulose [26]. Cellulolytic bacteria possess the ability to produce specific cellulases, enabling their conversion to valuable biofuels. The innovative enzyme combinations, microbial consortia, and bioengineering are crucial for successful biomass degradation [27, 28].

Despite decades of research, the systematic pretreatment and degradation of LCB, including GS, continues to be a major obstacle for twenty-first-century bio-refineries. The conversion of LCB into bioenergy involves employing pretreatment techniques such as physical, chemical, and biological methods. However, these methods have certain drawbacks because they are costly and cumbersome. Additionally, the development of highly efficient biocatalysts is a prerequisite for the production of biofuels [29–32]. The physical, chemical, and physico-chemical approaches for the utilization of waste biomass have proven ineffective due to their associated challenges and environmental issues; thus, a promising strategy of biological hydrolysis mediated by microbes is foreseen as a potential and promising alternative [33].

The enzymatic saccharification of LCB, facilitated by specific gut bacteria of animals, including snail emerges as a potentially attractive strategy from the sustainability perspective. The industrial use of lignocellulosic value-added products should consider enzymatic saccharification as a feasible strategy. Designing biologically distinct pathways to hydrolyze the LCB for a single cell is difficult. In contrast, bacterial consortia containing multiple species can balance two or more tasks simultaneously through synergistic mechanisms [34]. Therefore, splitting the biochemical functions by creating synthetic microbial consortia for a single-step cellulose conversion, where different microbial species and communities with specialized roles collaborate to enhance the bioconversion efficiency, seems to be a promising strategy [27]. This has inspired a fast-growing interest in engineering microbial consortia for biotechnology development. Thus, to increase the valorization of LCB, there is a dire

need to screen novel LCB, degrading microorganisms and creating effective microbial consortia [35].

In light of this objective, the present study aims to describe the saccharification of the chemically treated GS (CT-GS) by a bacterial consortium previously isolated from the gastro-intestinal tract of a giant African land snail [36]. The GS was pretreated with mild alkaline and acid solutions to enhance the overall hydrolytic efficiency of the consortium. The significance of pretreatment is that it was carried out at room temperature, and enzymatic digestibility was obtained through delignification of GS while rapid solubilization of the hemicellulose fraction improved hydrolysis of cellulose. Furthermore, the substrate (CT-GS) concentration and volume of consortia were optimized to improve the saccharification and fermentation potential of the bacterial consortium as well as yeast.

2 Materials and methods

2.1 Reagents and lignocellulosic substrates

The reagents like Sodium hydroxide (NaOH), D-glucose ($C_6H_{12}O_6$), 3,5-dinitrosalicylic acid (DNSA; $C_7H_4N_2O_7$), ammonium sulfate ($[NH_4]_2SO_4$), yeast extract, peptone, agar–agar, Potassium dichromate ($K_2Cr_2O_7$), Luria–Bertani broth (LB), disodium phosphate, were procured from the HiMedia (HiMedia Lab Pvt. Ltd., Mumbai, India) while the absolute ethanol, sulfuric acid (H_2SO_4), hydrochloric acid (HCL) were purchased from Thomas Baker (Thomas Baker Chemicals, Pvt. Ltd. Mumbai, India) and the SRL chemicals (Sisco Research Laboratories Pvt. Ltd. Mumbai, India), respectively. All chemicals and reagents were of the highest purity and analytical grade and prepared in sterile Milli-Q water unless otherwise mentioned. The lignocellulose substrates such as GS used in the study were collected from the Campus area (Latitude: 16.7050° N, Longitude: 74.2433° E) of Shivaji University, Vidyanagari, Kolhapur (MS), India.

2.2 Phylogeny of the microorganisms

The cellulose-degrading bacterial strains included *B. tequilensis* G9, *Achromobacter xylosoxidans* R2, *B. subtilis* R10, and *Bacillus* sp. R27 that were previously isolated from the gastro-intestinal tracts of giant African land snail, *Achatina fulica* [37]. The bacteria were identified through 16S rDNA gene sequencing using bacteria-specific primers 27F and 1492R [38]. The phylogenetic relationships were inferred through the alignment with nucleotide sequences of the closely related bacterial species retrieved from the GenBank. The phylogenetic trees were constructed by the neighbor-joining method using the Kimera-2 model in the MEGA X software, followed by annotation in the iTOL program

(https://itol.embl.de/) with 500 bootstrap values. A total of ten different consortia were formulated with these bacteria and evaluated for effective degradation of GS [36]. Based on our previous study, the most efficient bacterial consortium was further characterized here to valorize the enzymatic hydrolysis of alkaline acid–treated GS for the liberation of reducing sugars and their fermentation into bioethanol.

2.3 Pretreatment and preparation of substrates

The collected GS was cleaned and chopped with scissors to remove the soil and other impurities. Fifty grams (50 g) of the chopped GS was washed with distilled water (DW), and then treated with an alkaline solution of NaOH (1% in Milli-Q water w/v) for 24 h. Next, the substrates were continuously rinsed with DW to neutralize the pH. Once the pH of the filtrate was near neutral (~ 7), the substrates were subjected to acid treatment by immersing the GS in H_2SO_4 solution (10% in Milli-Q water v/v) for 24 h. Subsequently, the pretreated GS was rinsed repeatedly with DW till the pH of the filtrate was adjusted to pH 7.0. Thereafter, the pretreated substrates were air dried (at room temperature) at 30 ± 2 °C, ground in a pulverizer, and then sieved to achieve particles of uniform size (≤ 1 mm). The substrates were stored and preserved at room temperature until further use. The pretreated GS used as a substrate in the study is hereafter referred to as CT-GS. The visual macroscopic evaluation of GS after each stage of the pretreatment is shown in Fig. 1. The effect of the alkali and acid treatments was evident from the change in color as well as the morphology of the substrates. The overall methodological approach used in this study is presented in Fig. 1.

2.4 Characterization of the substrates

The untreated substrates (UT-GS) as well as CT-GS were characterized and assessed to determine the changes in chemical composition and structure of the substrates due to pretreatment processes. The change in functional groups was detected by Fourier transform infrared (FTIR) spectrometry using transmittance mode over the range of $400 - 4000$ cm^{-1} on an FTIR spectrometer (Bruker Alpha Shimadzu, Japan). For FTIR analysis, the samples were mixed with 200 mg of potassium bromide powder (KBr) and compressed to form a pellet (1–1.5 mm thickness) by applying pressure of 6–7 tons. Furthermore, the surface properties and crystallinity patterns of the UT-GS and CT-GS were detected through X-ray powder diffraction (XRD) at a scan rate of 12° min^{-1} and $2\theta = 5°–90°$ using Bruker's AXS Analytical Instruments (Bruker Pvt. Ltd., Germany). The crystallinity indices (CrI) of UT-GS and CT-GS were calculated using the following equation:
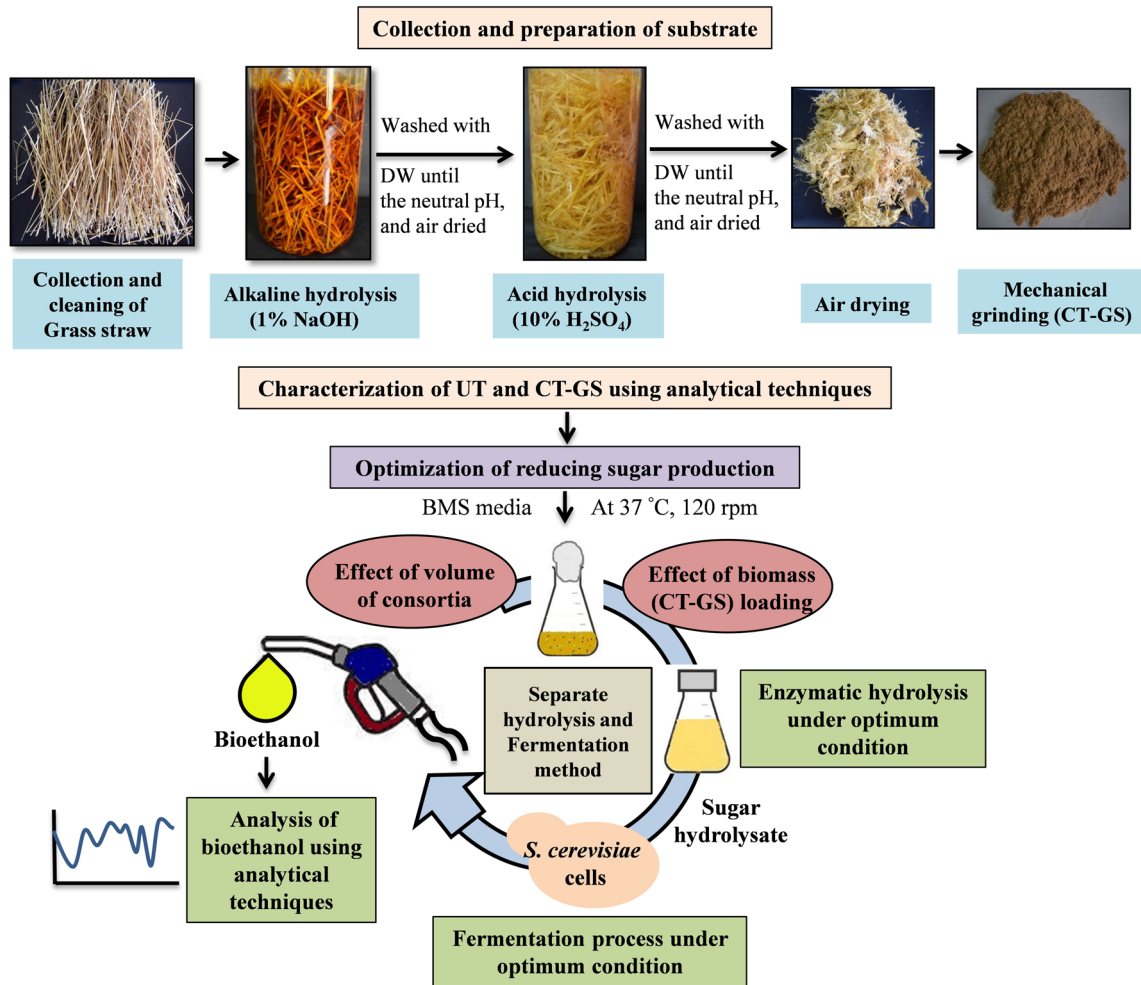
Fig. 1 An overview of the methodological approach used for the experimentation of the present study

$$CrI = (I_{002} - I_{001})/I_{002} \times 100 \qquad (1)$$

where I_{002} (2θ) and I_{001} (2θ) is the intensity of crystalline peaks and the amorphous peaks in XRD patterns respectively.

Similarly, the elemental composition of biomass was investigated and compared by energy dispersive X-ray (EDS) spectrometer using AztecLive EDS analysis software (Oxford Instruments, UK). The surface morphology of the UT-GS and CT-GS substrates was analyzed by field emission scanning electron microscopy (FESEM) using MIRA3 FESEM (TESCAN Bron, Czech Republic).

2.5 Effect of biomass loading and volume of consortia on reducing sugar production

The influence of biomass loading on sugar production using bacterial consortia was determined by varying the biomass loadings. To achieve this, the 250 mL Erlenmeyer flasks containing 100 mL of Berg minimal salt media (BMS) culture media were supplemented with varying biomass concentrations ranging from 0.5 to 4.0%. The media were inoculated with 1% consortium and incubated for 30 days in a rotary incubator shaking at 120 rpm at 37 °C. During the incubation period, sample aliquots of 2 mL were collected every 2 days to test the optimum concentration of the substrate required for maximum hydrolysis of CT-GS. The substrate hydrolysis was monitored by measuring the concentration of reducing sugars. To this end, sampled aliquots were centrifuged at 10,000 rpm for 10 min at 4 °C, and the supernatants obtained were assayed to estimate reducing sugar using the DNSA method [39]. In addition, the effect of the volume of consortium on substrate hydrolysis was also tested by using different volumes ranging from 0.5 to 4% of consortium in BMS medium. After inoculation, the culture flasks containing varying proportions of the bacterial consortium were incubated at 37 °C for 30 days in a rotary shaker. Similar to the influence of biomass loadings, sugar production was estimated by the DNSA method.

2.6 Bioethanol production

In this method, CT-GS was subjected to enzymatic saccharification by using bacterial consortium in BMS medium at the optimum conditions as determined in previous sections. The enzymatic hydrolysate of GS was concentrated to 5%, reducing sugar using a rotary evaporator (at 80 °C). The fermentation medium comprised of (g/L): 40; yeast extract, 5.0; $(NH4)_2SO_4$, 10.0; KH_2PO_4, 4.5; and $MgSO_4.7H_2O$, 1.0. The medium was inoculated with 4% (v/v) of 48-h-old seed culture of *S. cerevisiae*, then incubated at 30 °C and 120 rpm for fermentation. The experiments were carried out for 7 days at 30 °C. Ten milliters of the medium was sampled at regular intervals, centrifuged (10,000 rpm for 10 min), and filtered through 0.2 µM syringe filters for estimation of residual sugar contents and ethanol. The residual sugar was estimated by DNSA method [39] as prescribed earlier [36].

The supernatant obtained during the process of optimization was distilled using a distillation apparatus, and bioethanol was separated via the distillation process. For this, 3 mL of fermented sample was transferred to a round bottom flask and diluted with 30 mL Milli-Q water. The round bottom flasks were attached with condenser and collection flasks. The whole setup was placed on a heating mantle, and the water was circulated through the condenser. The temperature was maintained at 78–80 °C [Due to the difference in boiling point of water (100 °C) and ethanol (78.6 °C)] in the heating mantle. The vaporous was allowed to pass through the outlet port attached to the top. The evaporated fraction was then distilled, and the condensed sample was collected. Furthermore, the samples were subjected to distillation process, and then distillate was analyzed for ethanol content by the potassium di-chromate method. The ethanol was estimated calorimetrically [40] by dissolving 33.83 g of $K_2Cr_2O_7$ in 500 mL of DW followed by the addition of 325 mL of concentrated H_2SO_4 (36 N). The volume of solution was adjusted to 1000 mL with Milli-Q water, with a final normality of 0.23 N $K_2Cr_2O_7$ in solution. Finally, 25 mL of $K_2Cr_2O_7$ reagent (0.23 N) were mixed with 20 mL of distillate, and the samples were kept in a water bath at 60 °C for 20 min for the development of color. Afterwards, the reactions were cooled, followed by the measurement of optical density at 600 nm in a UV–Visible spectrophotometer (Eppendorf AG 22331 Biospectrometer, Hamburg, Germany).

2.7 Effect of physico-chemical parameters on ethanol production

The optimization of process conditions is paramount to obtain maximum ethanol yield. Different process parameters such as pH, temperature, yeast inoculum size, and fermentation period, were optimized for efficient bioconversion of CT-GS sugar hydrolysate into ethanol. The enzymatic hydrolysate of CT-GS was concentrated to a reducing sugar concentration

of 5% by evaporation in a rotary evaporator (80 °C). In order to study the effect of variation in pH of the medium, it was varied from 4.0 to 6.0 (increasing by 0.5 pH) with 1N hydrochloric acid (HCL) or alkali (1N NaOH) at RT under stirring conditions. Then media were inoculated with 6% (v/v) of *S. cerevisiae*, followed by incubation at 30 °C (120 rpm). Furthermore, the effect of temperature on ethanol fermentation was carried out by incubating the culture media at different temperatures, such as 25, 30, 35, and 40 °C, keeping pH and other conditions constant and optimum. Since the size of the yeast inoculum also significantly influences the rate of fermentation and ethanol yield, its optimization was carried out separately by varying the concentrations of *S. cerevisiae* in the range of 2 to 10% (v/v) in individual flasks and incubated at optimum pH and temperature.

Similarly, the fermentation of the reducing sugar hydrolysate was determined by varying fermentation periods ranging from 0 to 7 days, keeping all other parameters constant. During optimization, the culture supernatants (10 mL) were collected aseptically every 24 h for 7 days and centrifuged at 10,000 rpm for 10 min. The supernatants obtained were filtered through 0.2 µm syringe filters to collect the filtrate and subjected to a distillation process as mentioned in Sect. 2.6. The condensed samples were tested for bioethanol with $K_2Cr_2O_7$ reagent test [40]. The standard curves were plotted by using different concentrations ranging from 0 to 10% of the molecular grade ethanol solution. The cell biomass concentration was determined by the dry weight method [41]. For cell dry weight, 10 mL sample was collected and centrifuged at 10,000 rpm for 10 min in a pre-weighed tube, and then settled solids were washed with 10 mL of Milli-Q water. The tubes were dried overnight at 70 °C for 24 h and weighed again with weighing balance.

2.8 Confirmative analysis of bioethanol by gas chromatography-tandem mass spectroscopy and FTIR

The bioethanol obtained after separate hydrolysis and fermentation (SHF) process was analyzed by gas chromatography (GC–MS/MS) (Shimadzu, Japan) using SH-Rxi-5sil MS column (30 m × 0.25 µm). The column temperature during the program was 70 °C with the run time of 26 min. The injector temperature was maintained at 250 °C. The carrier gas was helium in the gas chromatography with the sample quantity of 1 µL at flow rate of 42 mL/min with spilt ratio of 1/25. The system was operated at electron ionization energy of 70 eV with 44 cm/sec of linear velocity. After comparing the respective retention times and mass spectra analyses with those of NIST14 library data (GC–MS system) and existing literature, the component identity was finally clarified. Furthermore, the bioethanol was confirmed using FTIR spectroscopy analysis to study the basic functional groups present in the sample.

2.9 Statistical analysis

All the experiments were performed in triplicates. To compare the data between UT-GS and CT-GS, a one-way analysis of variance (ANOVA) was conducted. Subsequently, multiple comparisons were carried out using the Tukey post-hoc test. A $p < 0.05$ was evaluated to consider statistical significance.

3 Results

3.1 Phylogenetic analysis of the consortium

The 16S rDNA sequencing revealed that bacterial consortium was composed of gram-positive (*Bacillus* spp.) as well as Gram-negative bacteria (*Achromobacter xylosoxidans*). Among the four bacterial strains, only one strain, *Achromobater xylosoxidans* R2, was gram-negative, belonging to the family Alcaligenaceae, while all other strains were affiliated with Gram-positive genera of *Bacillus*. The molecular homology inferred that the potential cellulose-degrading bacteria were *B. tequilensis* G9, *Achromobacter xylosoxidans* R2, *B. subtilis* R10, *and Bacillus* sp. R27. The phylogenetic tree (Fig. 2) demonstrated a > 99% similarity score of members of the bacterial consortium with closely related NCBI relatives.

3.2 Effect of the pretreatment process on the composition of grass straw

FTIR and XRD analysis The FTIR spectra of the untreated and chemically treated GS, as shown in Fig. 3a and Table 1, revealed noticeable changes in the composition of the substrates due to pretreatment processing. The FT-IR spectra of the UT-GS and CT-GS were dominated by the peaks at 3345 and 3399 cm^{-1}, reflecting the stretching vibrations of O–H stretching (hydrogen bond) [42] while the absorption bands at 2897 and 2354 cm^{-1} represented the CH, CH$_2$, or CH$_3$ stretching [43] and C-H stretch, C-H deformation of cellulose [44]. The wave numbers with peak intensities at 2132 and 2049 cm^{-1} were asfsociated with C=C stretch vibration of cellulose. The absence of the vibration peak at 1736 cm^{-1} in the CT-GS, was obvious for C–O stretching of methyl ester and carboxylic acid in pectin or acetyl groups in hemicelluloses [45]. Similarly, the intensity of the bands at 1432, 1374, 1375, 1646, and 1515 cm^{-1} was found to be associated with C–H in-plane deformation, C=C aromatic skeletal vibration, and aromatic ring vibration of lignin whereas decrease in intensity of both the peaks (at 1374 and 1515) in the CT-GS revealed the removal of lignin after the chemical treatment. The absorption peak that was absorbed at 1465 cm^{-1} reflected the C–H deformation of lignin [42]. The intensity of the prominent peak in IR spectra of UT-GS at 1315 cm^{-1} attributed to

Fig. 2 A phylogenetic analysis based on the 16S rDNA gene sequencing of the bacterial strains composing the lignocellulolytic consortium
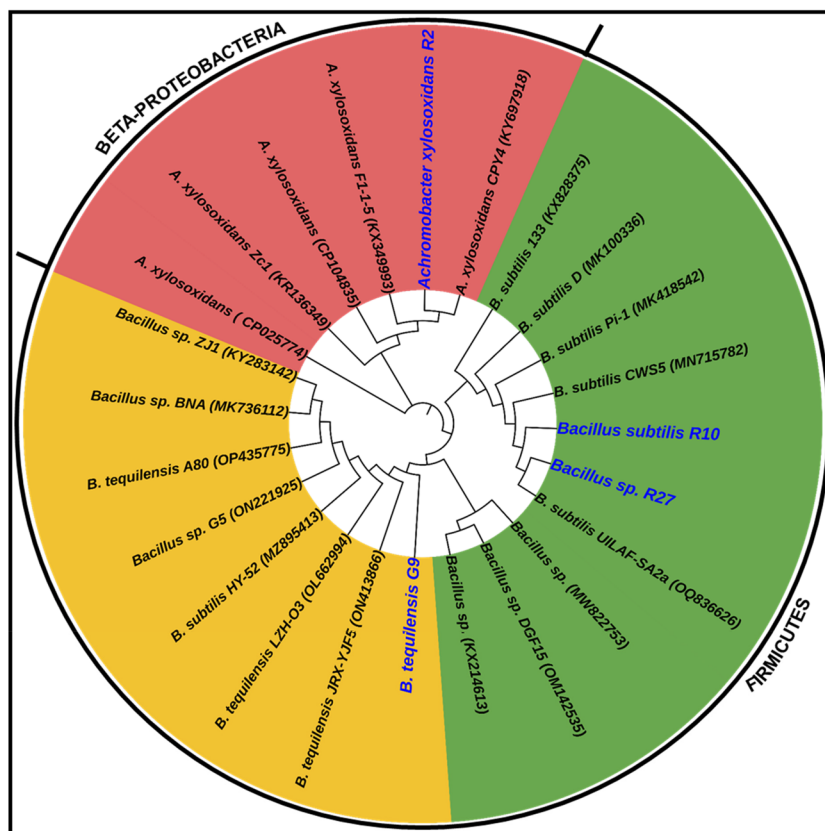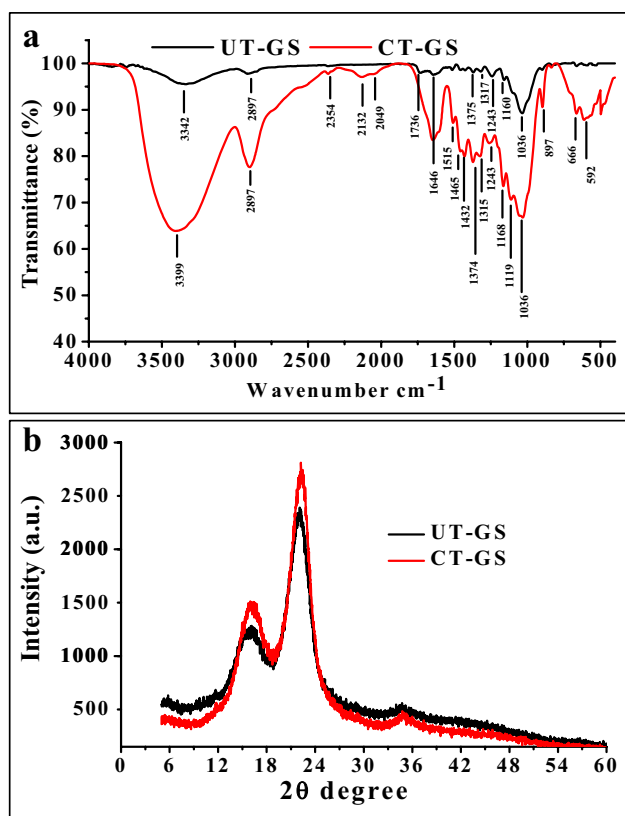
Fig. 3 Characterization of UT-GS and CT-GS. **a** FTIR, **b** XRD

–CH_2, C–H, or C–O of cellulose was found to increase after pretreatment (1317 cm^{-1}) [46]. The absorbance at 1243 cm^{-1} was associated with the C–O stretching in xylene of hemicellulose [47] while peaks at 1160 and 1168 cm^{-1} were assigned to C–O–C asymmetrical stretching in cellulose and hemicellulose [46]. The increase of the band intensities at 1036 and 897 cm^{-1} in the CT-GS indicated the aromatic C–H in-plane deformation [46] and typical β-1,4-glycosidic linkages of cellulose [48]. A detailed account of the changes observed in the chemical composition of the pretreated substrate is listed in Table 1, highlighting the effect of the combined alkaline-acid pretreatment on the bond's lignocellulosic material.

The X-ray diffraction crystallography of UT-GS and CT-GS exhibited two major peaks at 2θ around 22° and 16° representing crystalline cellulose and amorphous compounds, respectively (Fig. 3b). When compared to UT-GS, an increase in peak height at 22° was clearly observed in CT-GS, suggesting the higher exposure of crystalline cellulose. The CrI of UT-GS and CT-GS were 44.49 and 47.78%, respectively (Table 2).

EDS and FESEM analysis of biomass The EDS analyses indicated that UT-GS contained carbon (45.87%) and oxygen (27.19%) as dominant elements, indicating the carbon and oxygen atoms typically originated from the natural fiber (Fig. 4a). After pretreatment, the EDS spectra showed a higher percentage of carbon (78.39%) than oxygen (9.74%) in the CT-GS substrate (Fig. 4b). The morphological changes in

Table 1 FTIR-based identification of the altered functional groups in the GS due to alkali-acid pretreatment

| Frequency cm^{-1}	Functional group with type of vibrations	Corresponding biomass component	References
3300–3400	O–H stretching (hydrogen bond)	Cellulose	[32]
2897	CH, CH_2, or CH_3 stretching	Cellulose	[33]
2354	C–H stretch, C–H deformation	Cellulose	[34]
2132	C=C stretch vibration	Cellulose	[35]
2049	C=C stretch vibration	Cellulose	[35]
1736	C–O stretching of methyl ester and carboxylic acid in pectin or the acetyl group	Hemicellulose	[35]
1646	C=C aromatic skeletal vibration	Lignin	[32]
1515	Aromatic ring vibration	Lignin	[37]
1465	C–H deformation	Lignin	[32]
1432	C–H in-plane deformation	Lignin	[37]
1374, 1375	C–H deformation	Cellulose	[32]
1315, 1317	–CH_2, C–H or C–O of cellulose	Cellulose	[36]
1243	C–O stretching in xylene	Hemicellulose	[37]
1160, 1168	C–O–C asymmetrical stretching	Cellulose and hemicellulose	[36]
1036	aromatic C–H in-plane deformation	Cellulose	[36]
897	β–1,4–glycosidic linkages	Cellulose	[38]
666	C–OH bending	Cellulose	[35]
592	C–OH bending	Cellulose	[35]

Table 2 The crystalline index (CrI) of UT-GS and CT-GS estimated from the XRD analyses

LCB	I_{002} (2θ) intensity of crystalline peak	I_{001} (2θ) intensity of amorphous peak	CrI (%) Of LCB
UT-GS	22.21	16.12	44.49
CT-GS	22.21	16.12	47.78

the CT-GS substrate investigated through FESEM analysis (Fig. 4c) showed well-organized and unaffected surface of the untreated substrate, UT-GS. The smooth surfaces on the fibers indicated the lignin coverage, while the closed entire structure and intact plant cell wall with vascular structure indicated the recalcitrant nature observed in Fig. 4d. In contrast, the distorted surface and structure of the CT-GS revealed significant alteration caused by the chemical pretreatment. The surface of CT-GS turned rough and disorganized (Fig. 4e), which can be attributed to the hydrolysis of the amorphous regions of lignocellulose caused by the pretreatment processes.

3.3 Effect of biomass loading on reducing sugar production

In this study, different dosages of CT-GS were used to determine how biomass loading influences hydrolysis to produce reducing sugar. Figure 5a shows the interactive effect of biomass loading and incubation time on reducing sugar yield. Overall, a low yield of reducing sugar (5.71 ± 0.32–13.38 ± 0.20 μg/mL) was observed at lower biomass loadings (0.5–1%) after 4 days of incubation. However, the reducing sugar yield was found to consistently increase with higher biomass loadings (0.5–3%) up to 12 days. When the biomass loadings were further increased (3.5–4%), a decreasing trend in the reducing sugar production (159.69 ± 1.2–130.78 ± 1.0 μg/mL) was observed (Fig. 5a). In our study, a gradual increase in reducing sugar production from 57.91 ± 0.12–229.38 ± 1.42 μg/mL for 0.5–3% biomass loading was observed. Overall, the lowest sugar production was observed on 4th day of incubation
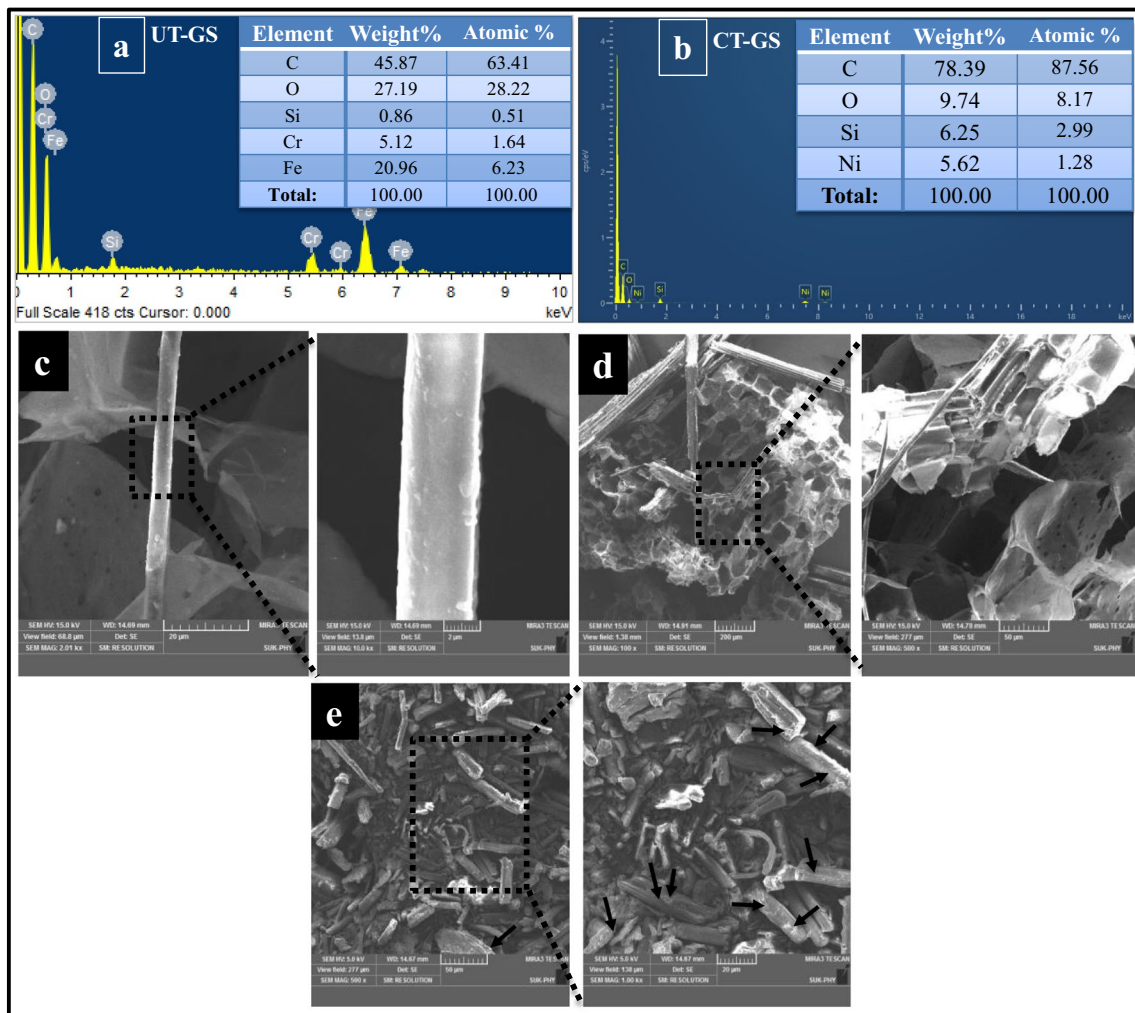
Fig. 4 The EDS of UT-GS (**a**) and CT-GS (**b**), and FE-SEM analysis of UT-GS (**c** and **d**) and CT-GS (**e**)
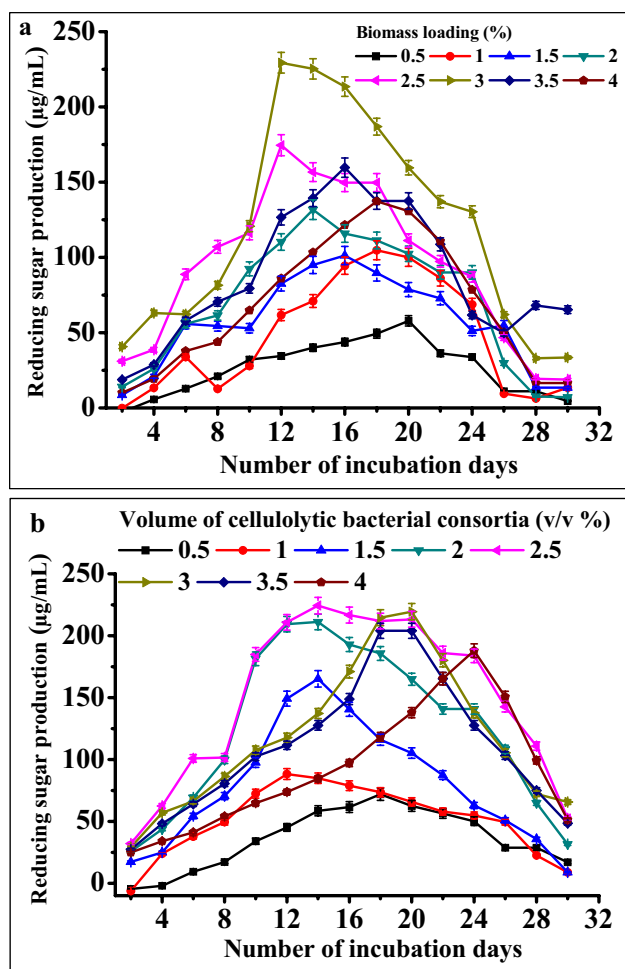
Fig. 5 The interactive effect of biomass loading (CT-GS) (**a**) and volume of cellulolytic bacterial consortia (**b**) on reducing sugar production over the incubation time of 30 days

with 0.5% biomass (Fig. 5a). The maximum reducing sugar yield of 229.38 ± 1.42 µg/mL at 3% biomass loading was obtained on 12+ day of incubation while its lowest sugar production (33.03 ± 0.11 µg/mL) was found on 28th day of incubation (Fig. 5a). The reducing sugar production from 16 to 30 days of incubation tends to reduce drastically in case of all biomass loadings. Thus, 3% (w/v) of CT-GS of biomass was the optimum substrate loading for the present system with 12 days of incubation for the production of reducing sugar of 229.38 ± 1.42 µg/mL.

3.4 Effect of consortia volume on reducing sugar production

To study the effect of volume of cellulolytic bacterial consortia, inoculum volumes ranging from 0.5 to 4% (v/v) were examined for reducing sugar productions (Fig. 5b). Maximum reducing sugar production of 224.33 ± 1.15 µg/

mL occurred with 2.5% (v/v) cellulolytic bacterial consortia after 14 days of incubation; however, further increase up to 4% (v/v) resulted in reduced sugar yield of 214.60 ± 1.0 to 187.94 ± 0.93 µg/mL from 18 to 24th day of incubation (Fig. 5b). The lowest inoculum size of 0.5% produced 71.94 ± 0.76 µg/mL of reducing sugar after 18 days of incubation, which could be attributed to the slow growth of the bacteria and reduced conversion of the substrates.

3.5 Optimization of bioethanol production

In this study, several process variables, such as pH, temperature, inoculum size, and fermentation period, were optimized. To this end, when the pH of culture media was varied in the range of pH 4–6 and studied by monitoring daily over the period of 7 days, the rate of ethanol production was found increased gradually from 0.88 ± 0.1 to $2.68 \pm 0.9\%$ (v/v) with increase in pH from 4 to 5.5 and declined thereafter up to $2.34 \pm 0.41\%$ (v/v) at pH 6 (Fig. 6a). The maximum ethanol production ($2.68 \pm 0.94\%$) (v/v) was attained at pH 5.5 after 4 days of fermentation (Fig. 6a).

Similarly, when the effect of temperature in the range of 25–40 °C (with an interval of 5 °C) on the ethanol production was studied, considerable variation in ethanol production with respect to incubation time was observed. The strain grew vigorously at 30 °C, yielding a higher ethanol yield of $2.10 \pm 0.92\%$ (v/v) after 5 days of incubation (Fig. 6b). After 5th day, a continuous decrease in the ethanol production ($0.14 \pm 0.25\%$) (v/v) was observed up to 7th day at all tested temperatures, being lowest at 35 °C. The optimization of the inoculum size of yeast is ideal to reduce the cost of cellulosic ethanol production.

To investigate the effect of inoculum size of the yeast on the production of ethanol, various volumes of yeast culture ranging from 2 to 10% (v/v) were added to the sugar hydrolysate-containing culture media. Figure 6c shows that the ethanol production increased from 1.60 ± 0.82 to $2.07 \pm 0.92\%$ (v/v) at 2 to 6% yeast inoculum, respectively. The ethanol production was enhanced ($3.02 \pm 0.94\%$) (v/v) with increasing amounts of the yeast culture of 8% after 5 days of incubation (Fig. 6c).

During the initial days of fermentation, cell biomass and ethanol concentrations showed an irregular trend, probably due to the adaptation of the yeast cells to the media conditions (Fig. 7). Thereafter, cell biomass grew quickly as a result of the fast utilization of nitrogen and glucose. A sharp increase in cell biomass and ethanol was observed between 1 and 3 days of incubation. After 3 days, biomass concentration remained largely steady, and fermentation was observed nearly at steady conditions. A prolonged incubation decreased both the cell biomass and ethanol production. In

Fig. 6 Optimization of ethanol production. **a** pH, **b** temperature, and **c** inoculum (*S. cerevisiae*) size
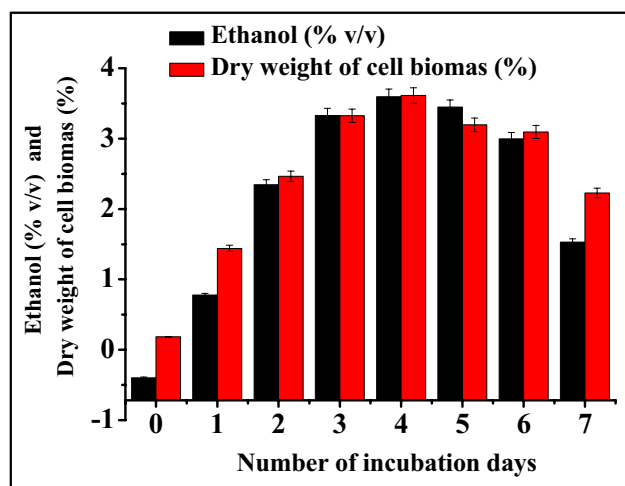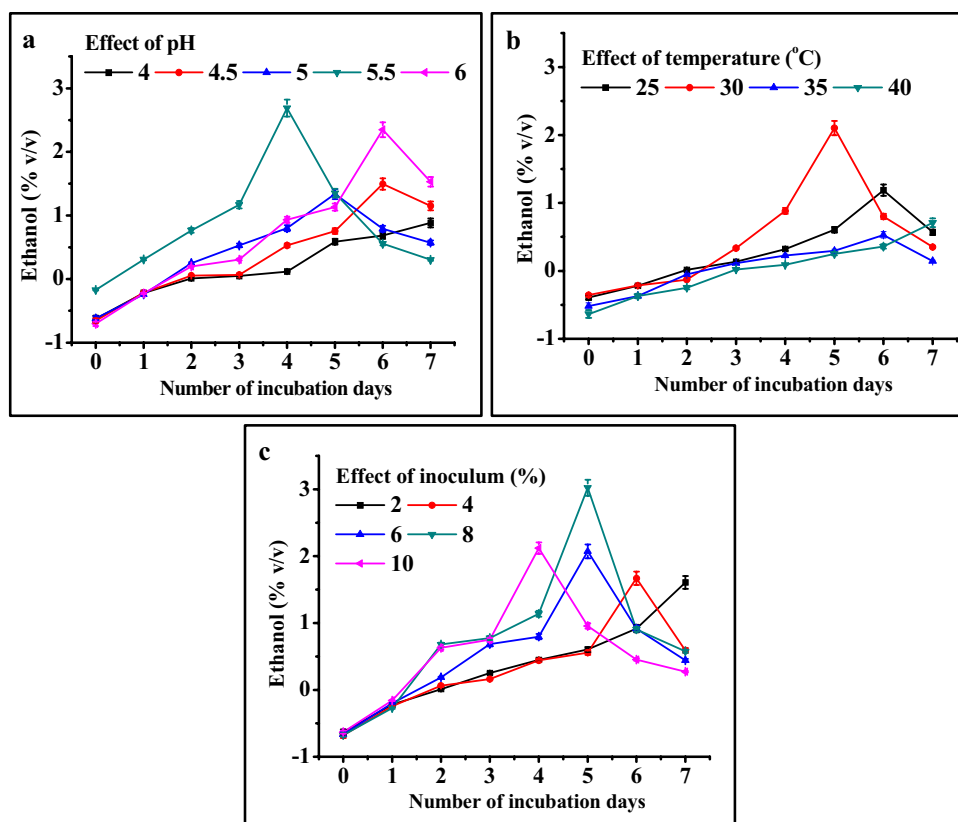

Fig. 7 Time-dependent ethanol production and dry weight of cell biomass

Table 3 GC–MS/MS-based identification of the products generated during fermentation

Peaks	Rt (min)	Area (%)	Retention index	Name of compound
1	1.045	96.54	463	Ethanol
2	1.256	1.17	597	1-Propanol, 2-methyl
3	1.631	2.28	697	1-Butanol, 3-methyl

3.6 Characterization of bioethanol

The chromatographic profile of the compounds derived from fermentation is shown in Figure S1 and the identified peaks are presented in Table 3. The peaks elucidating the fermentation were assigned to 1-Propanol, 2-methyl, and 1-Butanol, 3-methyl, with retention time (Rt) of 1.256 and 1.631 respectively. The peaks corresponding to ethanol showed Rt of 1.045 (Fig. S1). Thus, the mass spectrum of bioethanol monitored at 31 and 45 mz^{-1} ion fragments were the most abundant fragments for ethanol (Fig. S2). The FTIR results for the analyzed sample revealed typical bioethanol absorption bands (Fig. 8 and Table. S1). The broad absorption band at 3309 cm^{-1} corresponded to the O–H stretching vibration of alcohols, confirming the presence of the alcohol group [49]. The minor peak identified between 2914 cm^{-1} and 2853 cm^{-1} indicated the

terms of the incubation period, the cell biomass increased till 4th day, thereafter showed a decreased growth, which could be due to the limited nutrients and prolonged fermentation, thereby causing reduced ethanol yields (Fig. 7). However, it was observed that 3.59 ± 0.85% (v/v) maximum bioethanol production from CT-GS sugar hydrolysate was estimated within 4 days of incubation (Fig. 7).

O–H stretching and C-H-based alkane, respectively [50], whereas the weak intensity peaks at 2113 cm^{-1} could be attributed to –C $=$ C– (alkyne) [51]. In addition, the sharp peak at 1657 cm^{-1} corresponded to the water bands, which represents the bending vibration of the H–O–H angle and the stretching vibration of the O–H groups [52]. The small peaks at 1457 cm^{-1} represented the CH_2 and CH_3 groups [53]. In addition, C–O stretch at 1106 cm^{-1} confirmed the bonds in the structure of ethanol [54]. Furthermore, the characteristic bands that appeared around 1048 cm^{-1} were associated with the stretching vibration of C–OH [49] (Fig. 8).

4 Discussion

4.1 Phylogenetic analysis of the consortium

To date, several lignocellulose-degrading bacterial consortia have been isolated from the different environments [55, 56] but not from the gut system of animals, particularly snails. To this end, here we have formulated a bacterial consortium with efficient lignocellulose biodegradation capabilities from the gastro-intestinal tract of a giant African land snail, *Achatina fulica*, that predominantly feeds on plant matter [4, 37]. Moreover, the interest in the use of bacterial consortia for the valorization of lignocellulose has gained scientific interest in recent years [57, 58]. A significant feature of the consortia-mediated efficient biodegradation of lignocellulose could be attributed to the synergism and metabolic cooperation of these bacterial strains and their enzymes within the gut environments [59].
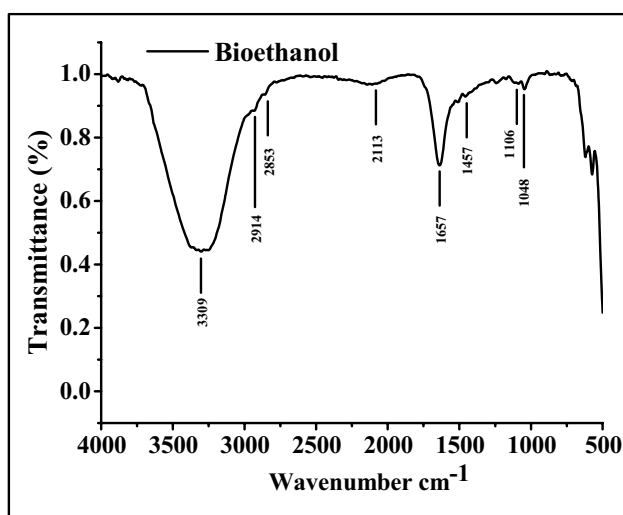

Fig. 8 FTIR spectra of the bioethanol produced from CT-GS after treatment with bacterial consortia

4.2 Effect of the pretreatment process on the composition of grass straw

The FTIR results indicate that pectin and hemicelluloses can be successfully removed using a combined alkaline-acid pretreatment. Therefore, it could be inferred that the significant differences observed between the chemical composition of UT-GS and CT-GS substrates were caused by the combined chemical pretreatment processes. The increase in CrI is proportional to the increase of crystalline cellulose in the total solid due to the removal of partial lignin, besides the amorphous contents of cellulose, hemicellulose, and other compounds [42, 60]. Moreover, lignin solubilization due to alkaline and acid treatments resulted in increased porosity and disintegration of the fiber matrix. In addition, the hydrogen bonding pattern between cellulose, hemicelluloses, and lignin components of the lignocellulosic polymer was typically disrupted by the pretreatment process [61]. Generally, the alkaline treatments are known to separate lignin from hemicellulose via OH radicals and dissolve hemicellulose and cellulose through the removal of hydrogen bonds between them, which in turn increases the degradation rate of the hemicellulose and lignin–complexes [62, 63]. This is well in agreement with our FTIR studies, where CT-GS showed functional groups with their corresponding biomass component (Fig. 3a). Thus, the main goal of pretreatment was to make the lignocellulosic fibers available for bacterial hydrolysis by increasing the porosity and exposing the cellulosic part for effective bioconversion. In other words, the morphological changes to CT-GS revealed the structure with increased exterior surface area to improve the enzymatic hydrolysis of the CT-GS by the consortium.

4.3 Effect of biomass loading on reducing sugar production

Biomass loading is one of the important variables that influence the reduction of sugar yield during enzymatic hydrolysis of LCB. The increasing substrate concentration also increases yield and hydrolysis rate; however, high substrate concentrations might hinder the overall hydrolysis process and adversely affect the yield due to feedback inhibition [64, 65]. The reduction in saccharification rate (reducing sugar production) at higher biomass loadings can be attributed to the limited stirring caused by a decrease in the aqueous phase and end product inhibition by the substrate concentration [24, 66].

The results of the current investigation are in congruence with the previous studies [65] that stated the concentration of reducing sugar increases proportionately with substrate loadings of 1 to 3% (w/v). However, the rise in the concentration of reducing sugar was insignificant when the substrate concentration was increased to 4%. Some studies have

shown that beyond certain concentrations and substrate loading, the rate of feedback inhibition by end products like cellobiose and glucose also increases, leading to reduced sugars production [67]. Our observations were in congruence with earlier studies [68, 69]. Since water serves as a reactant in hydrolysis reactions like the breakdown of glycosidic linkages, it is a crucial component for the diffusion of enzymes and sugar production in the lignocellulose bioconversion [70]. In the case of high-solid hydrolysis, lack of free water prevents diffusion of the end- products, while engaging the active sites of the enzymes with preoccupied substrates, thereby causing a strong inhibitory effect [71]. In the present study, after reaching the optimal conditions, reducing sugar yield started to fall after 20 days of incubation. Such effect can be attributed to end product inhibition caused by a high concentration of the product and mass transfer limitations within the reaction mixture due to the high viscosity of the slurry [70, 72].

4.4 Effect of consortia volume on reducing sugar production

The saccharification in terms of the concentration of reducing sugars released increased significantly during the initial period of incubation, being highest on the 14 days of culturing. After 14–24 days, the reducing sugar content was gradually reduced for 3–4% of the consortium. A reduction in the release of reducing sugars after 14 days could have occurred due to the consumption of the carbon source, leading to a lack of the available substrates for bacterial metabolism. In addition, the reduced sugars could be a result of the carbohydrate catabolism of the bacterial cells wherein they release the five- and six-carbon sugars from the cellulose and hemicellulose chains via enzymatic hydrolysis. These pentoses and hexoses are subsequently taken up and metabolized in the Embden-Meyerhof-Parnas pathway into two units of pyruvate, which then undergo oxidation to produce energy for the bacteria besides releasing CO_2 [73]. Furthermore, it is plausible to state that reduction in the number of bacteria during hydrolysis due to limited substrates or completion of the log phase of might have led to reduced sugar productions [74].

4.5 Optimization of bioethanol production

During fermentation, a number of variables influence the growth rate of yeast and ethanol yield [75]. The pH of the culture medium is paramount as it influences bacterial contamination, ethanol production, yeast growth, as well as generation of intermediate products. The observed production of ethanol from sugar hydrolysate was in congruence with previous studies, as yeast survival and development are largely impacted by pH levels between pH 2.75 to 4.25.

Since the ideal pH for fermentation processes of *S. cerevisiae* is 4.0–6.0 [76], our results are well in agreement with other reports that demonstrated bioethanol production at pH 5.5 with various substrates such as pretreated corn cob [77], pineapple peel [78], and *Moringa oleifera* seed husk [79].

As high temperatures are known to denature the tertiary structure of proteins and render them inactive, they become unfavorable for cell development and enzymes that govern microbial activity and, obviously for fermentation processes [80]. Our observations are aligned with other studies that also reported maximum fermentation of *Saccharum spontaneum* grass [81], wheat straw [82], rice straw [83], and bamboo hydrolysates [84] at temperatures between 20 to 33 °C by *S. cerevisiae* [85]. In the present study, the fermentation of CT-GS hydrolysate by *S. cerevisiae* was optimal at 30 °C, which is well in agreement with previous studies. Previously, many researchers have observed higher ethanol yields at 30 °C from the sugar hydrolysate of pretreated sugarcane leaves [86], wheat bran [87], and wheat straw [82] by using the SHF process.

In the context of the biorefinery, the bioethanol production obtained from the CT-GS is considerably higher when compared to the fermentation of wheat bran by *S. cerevisiae* [87]. Our results complement the observation reported by Farkas and colleagues, who used 10% yeast and found 4.5% bioethanol production from pretreated wheat bran after 7 days with a microbial consortium. The synthesis of ethanol is directly proportional to the inoculum size of the yeast. In other words, this states that increased cell concentration fastens the fermentation, allowing the cells to grow quickly and convert the available carbohydrates into bioethanol [88].

It could be observed that within first 3 days after inoculation, ethanol production as well as cell biomass showed a significant increase. Therefore, in the ethanol fermentation process, the value of ethanol produced reflects the number of living cell biomass. In addition, microorganism growth is influenced by fermentation duration. Shorter fermentation times result in ineffective fermentation due to insufficient microbial activity, whereas longer durations show harmful effects on microbial development. On the other hand, at lower temperatures, complete fermentation may be accomplished by extending the fermentation duration, resulting in the lowest ethanol production [88].

To date, few studies have investigated the suitability of various LCB substrates such as wheat straw [89], *Moringa oleifera* seeds husk [79], rice straw [42], bamboo [84], sugarcane leaves [86], sugarcane bagasse [90], rice husk [91], barley straw [92], rye straw [92], and Indian bamboo [93] for the production of bioethanol (Table S2). These studies indicate that the amount of sugar generated, the components employed in the fermentation process, and the amount of ethanol produced ultimately depend on the type of LCB used. As mentioned, the current study is in line with earlier

ones because majority of them have shown that the optimum bioethanol production was obtained in the range of 3–4 days of incubation period using sugar hydrolysate of different biomasses [42, 77, 94–96], etc. The high production of bioethanol within 3–4 days could be the result of the dissolved lignin and hemicellulose contents by the pretreatment processes before the enzymatic hydrolysis, leaving the readily usable and accessible sugars available for enzyme action and fermentation. Moreover, a combined pretreatment with dilute alkaline and acid solutions is largely appreciated for decomposition and reduced crystallinity of the lignocellulose besides the removal of enzyme inhibitors [20, 97]. Therefore, from the economic and practical viewpoints, a combined and mild pretreatment of the GS are recommended by the present study to achieve maximum bioethanol potentials through SHF processes.

Since *S. cerevisiae* has several important characteristics, including the capacity for rapid fermentation, genetic stability, resistance to low pH conditions, and tolerance to ethanol, and it is widely employed in many other biotechnological applications [98]. Recently, Douroua and his co-workers extracted and hydrolyzed polysaccharides of pomegranate residues to produce ethanol. The *S. cerevisiae* was reported to convert pomegranate residues derived reducing sugars into 9.7 g/L of bioethanol at pH 5.0 using 2.8 g/L of cell dry mass by solid-state fermentations [99]. On the contrary, the current study reports $3.59 \pm 0.85\%$ (v/v) of maximum bioethanol production at pH 5.5 on the by *S. cerevisiae* using 8% of yeast culture/inoculum by SHF process. In another study, oleaginous yeast strains were reported for lipids production using *Eucalyptus globulus* (hardwood), *Pinus radiata* (softwood), and rice hull hydrolysate [100, 101] as promising feedstocks for biodiesel production. The authors further observed that the yeast, *Meyerozyma guilliermondii* was able to consume total sugar within 50 to 90 h [101]; however, sugars present in rice hulls hydrolysate had a higher inhibitory effect on the fungal growth [100]. The fact that lignin and hemicellulose were dissolved by pretreatment procedures prior to enzymatic hydrolysis of CT-GS may have contributed to the high production of bioethanol in just 3–4 days by making the easily utilizable and accessible sugars available for fermentation and enzyme activities. Therefore, we state that the cellulolytic bacterial mediated degradation of CT-GS presents an economical and sustainable based strategy for the production of value-added products.

4.6 Characterization of bioethanol

In order to ascertain the potential products generated during the SHF process, we used GC–MS/MS that revealed the dominance of ethanol, which was in congruence with an agreement with a recent study [102]. Furthermore, FTIR was employed to assess the existence of functional gropes

of bioethanol obtained after the fermentation process. The FTIR spectrum showed that the characteristic peaks observed correspond to the alcohol group. The presence of the methyl groups was supported by the fact that alkaline pretreatments of LCB increase the production of methane in the fermentation media [62, 103]. The main advantage of SHF is characterized by two distinct processes: enzymatic hydrolysis of cellulose into fermentable sugars and the fermentation of the released sugars to produce bioethanol. In SHF, both hydrolysis and fermentation processes are performed at optimum conditions, which helps to achieve maximum yield of the products, besides avoiding the inhibitory action among the involved microbial species. Therefore, higher hydrolysis yields of fermentable sugars and better fermentation product yields often represent the outcomes of these independent optimization processes. Correspondingly, we report the successful production of bioethanol through SHF processes added by mild alkali-acid pretreatments of the GS to obtain higher ethanol concentration. Hence, this study showcased the utilization of straw-based agricultural wastes as a promising and renewable resource to produce bioethanol through a sustainable and green chemistry approach.

5 Conclusion

A successful and sustainable lignocellulosic biorefinery demands technological breakthroughs to address challenges like the requirement of multienzyme cocktails and the removal of lignin-blocking compounds. The primary shortcomings of existing microbial pretreatment techniques for lignocellulose materials include slow response, speed, and difficulties in practical application due to the recalcitrance imposed by lignin contents. In this study, the combination of biological and chemical methods proved significant for the efficient degradation of LCB and its subsequent fermentation into ethanol. A coupling effect can be produced by alkali-acid pretreatment and microbial consortia degradation. For GS, a combined treatment approach followed by consortia-mediated enzymatic hydrolysis proved to be an efficient method to produce higher concentrations of reducing sugars that can be fermented into bioethanol via separate saccharification and fermentation strategies using *S. cerevisiae* as the fermentation catalyst. The changes in the operational pH, temperature, and inoculum size caused changes in ethanol production, signifying theat optimization is important for higher yields. In conclusion, the combined chemical pretreatment enhanced the GS saccharification and fermentation, suggesting a potential strategy for higher ethanol yields. However, a thorough economic and process design is necessary to establish an industrially appropriate production strategy that will alleviate our energy problems by generating more ethanol in a steady manner.

Author contribution Priyadarshani S. Sadalage: project administration, methodology, investigation, validation, visualization, writing—original draft and editing. Mudasir A. Dar: formal analysis, data curation, writing—review and editing. Ana Cláudia Paiva-Santos: formal analysis. Kiran D. Pawar: conceptualization, supervision, validation and writing—review and editing.

Data availability All data generated or analyzed during this study are included in this published article [and its supplementary information files].

Declarations

Ethics approval This study does not contain any experiments with human participants or animals.

Consent for publication All the authors agree with consent to publication, and the current article does not contain data from any individual person.

Conflict of interest The authors declare no competing interests.

References

1. Hoang T-D, Nghiem N (2021) Recent developments and current status of commercial production of fuel ethanol. Fermentation 7:1–18. https://doi.org/10.3390/fermentation7040314
2. Muktham R, Bhargava SK, Bankupalli S, Ball SA (2016) A review on 1st and 2nd generation bioethanol production-recent progress. J Sustain Bioenergy Syst 06:72–92. https://doi.org/10.4236/jsbs.2016.63008
3. Mujtaba M, Fernandes Fraceto L, Fazeli M et al (2023) Lignocellulosic biomass from agricultural waste to the circular economy: a review with focus on biofuels, biocomposites and bioplastics. J Clean Prod 402:136815. https://doi.org/10.1016/j.jclepro.2023.136815
4. Dar MA, Pawar KD, Pandit RS (2018) Prospecting the gut fluid of giant African land snail, Achatina fulica for cellulose degrading bacteria. Int Biodeterior Biodegrad 126:103–111. https://doi.org/10.1016/j.ibiod.2017.10.006
5. Ma Y, Shen Y, Liu Y (2020) State of the art of straw treatment technology: challenges and solutions forward. Bioresour Technol 313:123656. https://doi.org/10.1016/j.biortech.2020.123656
6. Sun LN, Ma XY, Liu KB et al (2018) A review on research advances on microbial treatment and strengthening techniques of crop straw. J Shenyang Univ Nature Sci 30:188–195. https://doi.org/10.16103/j.cnki.21-1583/n.2018.03.004
7. Sun Y, Cheng J (2002) Hydrolysis of lignocellulosic materials for ethanol production: a review. Bioresour Technol 83:1–11. https://doi.org/10.1016/S0960-8524(01)00212-7
8. Howard RL, Abotsi E, Van Rensburg ELJ, Howard S (2003) Lignocellulose biotechnology: issues of bioconversion and enzyme production. African J Biotechnol 2:602–619. https://doi.org/10.5897/ajb2003.000-1115
9. Gaballah ES, Abomohra AEF, Xu C et al (2020) Enhancement of biogas production from rape straw using different co-pretreatment techniques and anaerobic co-digestion with cattle manure. Bioresour Technol 309:123311. https://doi.org/10.1016/j.biortech.2020.123311
10. He C, Zhang Z, Xie C et al (2021) Transformation behaviors and environmental risk assessment of heavy metals during resource recovery from Sedum plumbizincicola via hydrothermal liquefaction. J Hazard Mater 410:124588. https://doi.org/10.1016/j.jhazmat.2020.124588
11. Li X, Zhang X, Shao S et al (2018) Catalytic upgrading of pyrolysis vapor from rape straw in a vacuum pyrolysis system over La/HZSM-5 with hierarchical structure. Bioresour Technol 259:191–197. https://doi.org/10.1016/j.biortech.2018.03.046
12. Tocco D, Carucci C, Monduzzi M et al (2021) Recent developments in the delignification and exploitation of grass lignocellulosic biomass. ACS Sustain Chem Eng 9:2412–2432. https://doi.org/10.1021/acssuschemeng.0c07266
13. Poolakkalody NJ, Thattantavide A, Manisseri C (2022) Evaluating the biofuel potential of perennial grass, Pennisetum polystachion based on aqueous 1-ethyl, 3-methylimidazolium acetate ([EMIM][Ac]) pretreatment. Biomass Convers Biorefinery 13:15845–15859. https://doi.org/10.1007/s13399-021-02166-6
14. Vogel J (2008) Unique aspects of the grass cell wall. Curr Opin Plant Biol 11:301–307. https://doi.org/10.1016/j.pbi.2008.03.002
15. Saini JK, Saini R, Tewari L (2015) Lignocellulosic agriculture wastes as biomass feedstocks for second-generation bioethanol production : concepts and recent developments. 3 Biotech 5:337–353. https://doi.org/10.1007/s13205-014-0246-5
16. Bhattacharya AS, Bhattacharya A, Pletschke BI (2015) Synergism of fungal and bacterial cellulases and hemicellulases: a novel perspective for enhanced bio-ethanol production. Biotechnol Lett 37:1117–1129. https://doi.org/10.1007/s10529-015-1779-3
17. Buchspies B, Kaltschmitt M, Junginger M (2020) Straw utilization for biofuel production: a consequential assessment of greenhouse gas emissions from bioethanol and biomethane provision with a focus on the time dependency of emissions. GCB Bioenergy 12:789–805. https://doi.org/10.1111/gcbb.12734
18. Kassaye S, Pant KK, Jain S (2017) Hydrolysis of cellulosic bamboo biomass into reducing sugars via a combined alkaline solution and ionic liquid pretreament steps. Renew Energy 104:177–184. https://doi.org/10.1016/j.renene.2016.12.033
19. Mankar AR, Pandey A, Modak A, Pant KK (2021) Pretreatment of lignocellulosic biomass: a review on recent advances. Bioresour Technol 334:125235. https://doi.org/10.1016/j.biortech.2021.125235
20. Zabed HM, Akter S, Dar MA et al (2023) Enhanced fermentable sugar production in lignocellulosic biorefinery by exploring a novel corn stover and configuring high-solid pretreatment conditions. Bioresour Technol 386:129498. https://doi.org/10.1016/j.biortech.2023.129498
21. Khan MFS, Akbar M, Xu Z, Wang H (2021) A review on the role of pretreatment technologies in the hydrolysis of lignocellulosic biomass of corn stover. Biomass Bioenerg 155:106276. https://doi.org/10.1016/j.biombioe.2021.106276
22. Jönsson LJ, Martín C (2016) Pretreatment of lignocellulose: formation of inhibitory by-products and strategies for minimizing their effects. Bioresour Technol 199:103–112. https://doi.org/10.1016/j.biortech.2015.10.009
23. Zhao L, Sun ZF, Zhang CC et al (2022) Advances in pretreatment of lignocellulosic biomass for bioenergy production: challenges and perspectives. Bioresour Technol 343:126123. https://doi.org/10.1016/j.biortech.2021.126123
24. Chen H, Liu J, Chang X et al (2017) A review on the pretreatment of lignocellulose for high-value chemicals. Fuel Process Technol 160:196–206. https://doi.org/10.1016/j.fuproc.2016.12.007

25. de Souza WR (2013) Microbial degradation of lignocellulosic biomass. In: Sustainable degradation of lignocellulosic biomass - Techniques, Applications and Commercialization. Intech, Croatia. 207–247. https://doi.org/10.5772/54325

26. Pathak VM, Navneet (2017) Review on the current status of polymer degradation: a microbial approach. Bioresour Bioprocess 4:1–31 https://doi.org/10.1186/s40643-017-0145-9

27. Rosnow JJ, Anderson LN, Nair RN et al (2017) Profiling microbial lignocellulose degradation and utilization by emergent omics technologies. Crit Rev Biotechnol 37:626–640. https://doi.org/10.1080/07388551.2016.1209158

28. Malgas S, Thoresen M, van Dyk JS, Pletschke BI (2017) Time dependence of enzyme synergism during the degradation of model and natural lignocellulosic substrates. Enzyme Microb Technol 103:1–11. https://doi.org/10.1016/j.enzmictec.2017.04.007

29. Arora A, Nandal P, Singh J, Verma ML (2020) Nanobiotechnological advancements in lignocellulosic biomass pretreatment. Mater Sci Energy Technol 3:308–318. https://doi.org/10.1016/j.mset.2019.12.003

30. Singh N, Dhanya BS, Verma ML (2020) Nano-immobilized biocatalysts and their potential biotechnological applications in bioenergy production. Mater Sci Energy Technol 3:808–824. https://doi.org/10.1016/j.mset.2020.09.006

31. Verma ML, Azmi W, Kanwar SS (2011) Enzymatic synthesis of isopropyl acetate by immobilized Bacillus cereus lipase in organic medium. Enzyme Res 2011:7. https://doi.org/10.4061/2011/919386

32. Verma ML, Puri M, Barrow CJ (2016) Recent trends in nanomaterials immobilised enzymes for biofuel production. Crit Rev Biotechnol 36:108–119. https://doi.org/10.3109/07388551.2014.928811

33. Dar MA, Shaikh AF, Pawar KD et al (2021) Evaluation of cellulose degrading bacteria isolated from the gut-system of cotton bollworm, Helicoverpa armigera and their potential values in biomass conversion. PeerJ 9:e11254. https://doi.org/10.7717/peerj.11254

34. Mesbah NM (2022) Industrial biotechnology based on enzymes from extreme environments. Front Bioeng Biotechnol 10:1–16. https://doi.org/10.3389/fbioe.2022.870083

35. Mee MT, Wang HH (2012) Engineering ecosystems and synthetic ecologies. Mol Biosyst 8:2470–2483. https://doi.org/10.1039/c2mb25133g

36. Sadalage PS, Dar MA, Chavan AR, Pawar KD (2020) Formulation of synthetic bacterial consortia and their evaluation by principal component analysis for lignocellulose rich biomass degradation. Renew Energy 148:467–477. https://doi.org/10.1016/j.renene.2019.10.053

37. Dar MA, Pawar KD, Jadhav JP, Pandit RS (2015) Isolation of cellulolytic bacteria from the gastro-intestinal tract of Achatina fulica (Gastropoda: Pulmonata) and their evaluation for cellulose biodegradation. Int Biodeterior Biodegrad 98:73–80. https://doi.org/10.1016/j.ibiod.2014.11.016

38. Weisburg WG, Barns SM, Pelletier DA, Lane DJ (1991) 16S ribosomal DNA amplification for phylogenetic study. J Bacteriol 173:697–703. https://doi.org/10.1128/jb.173.2.697-703.1991

39. Miller GL (1959) Use of dinitrosalicylic acid reagent for determination of reducing sugar. Anal Chem 31:426–428. https://doi.org/10.1021/ac60147a030

40. Caputi J, Ueda M, Brown T (1968) Spectrophotometric determination of ethanol in wine. AM J Enol Vitic 19:160–165

41. Kasemets K, Nisamedtinov I, Laht TM et al (2007) Growth characteristics of Saccharomyces cerevisiae S288C in changing environmental conditions: auxo-accelerostat study. Antonie Van Leeuwenhoek 92:109–128. https://doi.org/10.1007/s10482-007-9141-y

42. Phitsuwan P, Permsriburasuk C, Baramee S et al (2017) Structural analysis of alkaline pretreated rice straw for ethanol production. Int J Polym Sci 2017:9

43. Luna IZ, Dam KC, Chowdhury AMS et al (2015) Physical and thermal characterization of alkali treated rice husk reinforced polypropylene composites. Adv Mater Sci Eng 2015:7. https://doi.org/10.1155/2015/907327

44. Xu F, Yu J, Tesso T et al (2013) Qualitative and quantitative analysis of lignocellulosic biomass using infrared techniques: A mini-review. Appl Energy 104:801–809. https://doi.org/10.1016/j.apenergy.2012.12.019

45. Salim RM, Asik J, Sarjadi MS (2021) Chemical functional groups of extractives, cellulose and lignin extracted from native Leucaena leucocephala bark. Wood Sci Technol 55:295–313. https://doi.org/10.1007/s00226-020-01258-2

46. Teli MD, Jadhav AC (2016) Effect of alkali treatment on the properties of Agave augustifolia v. marginata fibre. Int Res J Eng Technol 03:2754–2761

47. Danso B, Ali SS, Xie R, Sun J (2022) Valorisation of wheat straw and bioethanol production by a novel xylanase- and cellulase-producing Streptomyces strain isolated from the wood-feeding termite, microcerotermes species. Fuel 310:122333. https://doi.org/10.1016/j.fuel.2021.122333

48. Vora RS, Shah YD (2015) Production of micro crystalline cellulose from corn husk and its evaluation as pharmaceutical excipient. Int J Res Sci Innov 2:69–74

49. Chilakamarry CR, Mimi Sakinah AM, Zularism AW et al (2022) Glycerol waste to bio-Ethanol: optimization of fermentation parameters by the taguchi method. J Chem 2022:1–11. https://doi.org/10.1155/2022/4892992

50. Nagenderan S, Rajamamundi P, Chandran M, Gopinath KP (2020) Bioethanol from Moringa olefira and Pithecellobium dulce leafs: production and characterization. Energy Sources, Part A Recover Util Environ Eff 42:1–7. https://doi.org/10.1080/15567036.2019.1587055

51. Sanjivkumar M, Brindhashini A, Deivakumari M et al (2017) Investigation on saccharification and bioethanol production from pretreated agro-residues using a mangrove associated actinobacterium Streptomyces variabilis (MAB3). Waste Biomass Valorization 9:969–984. https://doi.org/10.1007/s12649-017-9886-0

52. Alminderej FM, Hamden Z, El-Ghoul Y et al (2022) Impact of calcium and nitrogen addition on bioethanol production by S. cerevisiae fermentation from date by-products: physicochemical characterization and technical design. Fermentation 8:1–17. https://doi.org/10.3390/fermentation8110583

53. Cunhaa CBD, Lopes PP, Mayer FD, Hoffmann R (2018) Assessment of chemical and mechanical properties of polymers aiming to replace the stainless steel in distillation column. Mater Res 21:1. https://doi.org/10.1590/1980-5373-MR-2017-0679

54. Gebrehiwot G, Jabasingh SA, Yimam A (2017) Production of cellulosic ethanol from wood sawdust by sulphuric acid Hydrolysis. J Pet Eng Technol 7:30–35

55. Díaz Rodríguez CA, Díaz-García L, Bunk B et al (2022) Novel bacterial taxa in a minimal lignocellulolytic consortium and their potential for lignin and plastics transformation. ISME Commun 2:1–12. https://doi.org/10.1038/s43705-022-00176-7

56. Weiss ND, Felby C, Thygesen LG (2019) Enzymatic hydrolysis is limited by biomass-water interactions at high-solids: Improved performance through substrate modifications. Biotechnol Biofuels 12:1–13. https://doi.org/10.1186/s13068-018-1339-x

57. Peng X, Wilken SE, Lankiewicz TS et al (2021) Genomic and functional analyses of fungal and bacterial consortia that enable lignocellulose breakdown in goat gut microbiomes. Nat Microbiol 6:499–511. https://doi.org/10.1038/s41564-020-00861-0

58. Cortes-Tolalpa L, Salles JF, van Elsas JD (2017) Bacterial synergism in lignocellulose biomass degradation - complementary roles of degraders as influenced by complexity of the carbon source. Front Microbiol 8:1–14. https://doi.org/10.3389/fmicb.2017.01628

59. Cao Z, Yan W, Ding M, Yuan Y (2022) Construction of microbial consortia for microbial degradation of complex compounds. Front Bioeng Biotechnol 10:1051233. https://doi.org/10.3389/fbioe.2022.1051233

60. Wang Q, Hu J, Shen F et al (2016) Pretreating wheat straw by the concentrated phosphoric acid plus hydrogen peroxide (PHP): investigations on pretreatment conditions and structure changes. Bioresour Technol 199:245–257. https://doi.org/10.1016/j.biortech.2015.07.112

61. Kumar S, Gandhi P, Yadav M et al (2019) Weak alkaline treatment of wheat and pearl millet straw for enhanced biogas production and its economic analysis. Renew Energy 139:753–764. https://doi.org/10.1016/j.renene.2019.02.133

62. Schroeder BG, İstanbullu HB, Schmidt M et al (2023) Effect of alkaline and mechanical pretreatment of wheat straw on enrichment cultures from Pachnoda marginata larva gut. Fermentation 9:1–20. https://doi.org/10.3390/fermentation9010060

63. Bali G, Meng X, Deneff JI et al (2015) The effect of alkaline pretreatment methods on cellulose structure and accessibility. ChemSusChem Commun 8:275–279. https://doi.org/10.1002/cssc.201402752

64. Chen HZ, Liu ZH (2017) Enzymatic hydrolysis of lignocellulosic biomass from low to high solids loading. Eng Life Sci 17:489–499. https://doi.org/10.1002/elsc.201600102

65. Subhedar PB, Babu NR, Gogate PR (2015) Intensification of enzymatic hydrolysis of waste newspaper using ultrasound for fermentable sugar production. Ultrason Sonochem 22:326–332. https://doi.org/10.1016/j.ultsonch.2014.07.005

66. Singhania RS, Patel AK, Raj T et al (2022) Advances and challenges in biocatalysts application for high solid-loading of biomass for 2nd generation bio-ethanol production. Catalysts 12:17. https://doi.org/10.3390/catal12060615

67. Zhong R, Morrison WH, Himmelsbach DS et al (2000) Essential role of caffeoyl coenzyme A O-methyltransferase in lignin biosynthesis in woody poplar plants. Plant Physiol 124:563–577. https://doi.org/10.1104/pp.124.2.563

68. Mardawati E, Werner A, Bley T et al (2014) The enzymatic hydrolysis of oil palm empty fruit bunches to xylose. J Japan Inst Energy 93:973–978. https://doi.org/10.3775/jie.93.973

69. Han L, Feng J, Zhang S et al (2012) Alkali pretreated of wheat straw and its enzymatic hydrolysis. Brazilian J Microbiol 43:53–61. https://doi.org/10.1590/S1517-83822012000100006

70. Da Silva ASA, Espinheira RP, Teixeira RSS et al (2020) Constraints and advances in high-solids enzymatic hydrolysis of lignocellulosic biomass: a critical review. Biotechnol Biofuels 13:1–28. https://doi.org/10.1186/s13068-020-01697-w

71. Hsieh CC, Cannella D, Jørgensen H et al (2014) Cellulase inhibition by high concentrations of monosaccharides. J Agric Food Chem 62:3800–3805

72. Fabbrizi G, Giannoni T, Lorenzi L et al (2022) High solid and low cellulase enzymatic hydrolysis of cardoon stems pretreated by acidified γ-valerolactone/water solution. Energies 15:1–12. https://doi.org/10.3390/en15072600

73. Dar MA, Dhole NP, Xie R et al (2021) Valorization potential of a novel bacterial strain, Bacillus altitudinis RSP75, towards lignocellulose bioconversion: an assessment of symbiotic bacteria from the stored grain pest, Tribolium castaneum. Microorganisms 9:1–24. https://doi.org/10.3390/microorganisms9091952

74. Ojewumi ME, Obielue BI, Emetere ME et al (2018) Alkaline pretreatment and enzymatic hydrolysis of waste papers to fermentable sugar. J Ecol Eng 19:211–217. https://doi.org/10.12911/22998993/79404

75. Mohd Azhar SH, Abdulla R, Jambo SA et al (2017) Yeasts in sustainable bioethanol production: a review. Biochem Biophys Reports 10:52–61. https://doi.org/10.1016/j.bbrep.2017.03.003

76. Johnston NR, Nallur S, Gordon PB et al (2020) Genome-wide identification of genes involved in general acid stress and fluoride toxicity in Saccharomyces cerevisiae. Front Microbiol 11:1–11. https://doi.org/10.3389/fmicb.2020.01410

77. Antunes FAF, Freitas JBF, Prado CA et al (2023) Valorization of corn cobs for xylitol and bioethanol production through column reactor process. Energies 16:1–15. https://doi.org/10.3390/en16134841

78. Antonio RMDR, Dela Cruz CAA, Quinto A Jr et al (2015) Bioethanol production from pineapple (Ananas comosus) peelings using Saccharomyces cerevisiae as fermenting yeast with focus on fermentation pH. Int J Eng Res Technol 4:356–360

79. Ali EN, Kemat SZ (2017) Bioethanol produced from Moringa oleifera seeds husk. IOP Conf Ser Mater Sci Eng 206:1–11. https://doi.org/10.1088/1757-899X/206/1/012019

80. Phisalaphong M, Srirattana N, Tanthapanichakoon W (2006) Mathematical modeling to investigate temperature effect on kinetic parameters of ethanol fermentation. Biochem Eng J 28:36–43. https://doi.org/10.1016/j.bej.2005.08.039

81. Sharma D, Joshi B, Bhatt MR et al (2015) Isolation of cellulolytic organisms from the gut contents of termites native to nepal and their utility in saccharification and fermentation of lignocellulosic biomass. J Biomass Biofuel 2:11–20. https://doi.org/10.11159/jbb.2015.002

82. Chen J, Wang X, Zhang B et al (2021) Integrating enzymatic hydrolysis into subcritical water pretreatment optimization for bioethanol production from wheat straw. Sci Total Environ 770:145321. https://doi.org/10.1016/j.scitotenv.2021.145321

83. Chuetor S, Panakkal EJ, Ruensodsai T et al (2022) Improvement of enzymatic saccharification and ethanol production from rice straw using recycled ionic liquid: the effect of anti-solvent mixture. Bioengineering 9:1–15. https://doi.org/10.3390/bioengineering9030115

84. Wi SG, Lee DS, Nguyen QA, Bae HJ (2017) Evaluation of biomass quality in short-rotation bamboo (Phyllostachys pubescens) for bioenergy products. Biotechnol Biofuels 10:1–11. https://doi.org/10.1186/s13068-017-0818-9

85. Lip KYF, García-Ríos E, Costa CE et al (2020) Selection and subsequent physiological characterization of industrial Saccharomyces cerevisiae strains during continuous growth at sub-and- supra optimal temperatures. Biotechnol Reports 26:e00462. https://doi.org/10.1016/j.btre.2020.e00462

86. Dodo CM, Mamphweli S, Okoh O (2017) Bioethanol production from lignocellulosic sugarcane leaves and tops. J Energy South Africa 28:1–11. https://doi.org/10.17159/2413-3051/2017/v28i3a2354

87. Farkas C, Rezessy-Szabó JM, Gupta VK et al (2019) Microbial saccharification of wheat bran for bioethanol fermentation. J Clean Prod 240:118269. https://doi.org/10.1016/j.jclepro.2019.118269

88. Zabed H, Faruq G, Sahu JN et al (2014) Bioethanol production from fermentable sugar juice. Sci World J 2014:1–11. https://doi.org/10.1155/2014/957102

89. Qiu J, Ma L, Shen F et al (2017) Pretreating wheat straw by phosphoric acid plus hydrogen peroxide for enzymatic saccharification and ethanol production at high solid loading. Bioresour Technol 238:174–181. https://doi.org/10.1016/j.biortech.2017.04.040

90. de Carvalho DM, de Queiroz JH, Colodette JL (2016) Assessment of alkaline pretreatment for the production of bioethanol from eucalyptus, sugarcane bagasse and sugarcane straw. Ind Crops Prod 94:932–941. https://doi.org/10.1016/j.indcrop.2016.09.069

91. ArismendyPabón AM, Felissia FE, Mendieta CM et al (2020) Improvement of bioethanol production from rice husks. Cellul Chem Technol 54:689–698. https://doi.org/10.35812/CelluloseChemTechnol.2020.54.68

92. Hawrot-Paw M, Koniuszy A, Zając G et al (2020) Production of second generation bioethanol from straw during simultaneous microbial saccharification and fermentation. Arch Environ Prot 46:47–52. https://doi.org/10.24425/aep.2020.132525

93. Sindhu R, Kuttiraja M, Binod P et al (2014) Bioethanol production from dilute acid pretreated Indian bamboo variety (Dendrocalamus

sp.) by separate hydrolysis and fermentation. Ind Crop Prod 52:169–176. https://doi.org/10.1016/j.indcrop.2013.10.021

94. Dahnum D, Tasum SO, Triwahyuni E et al (2015) Comparison of SHF and SSF processes using enzyme and dry yeast for optimization of bioethanol production from empty fruit bunch. Energy Procedia 68:107–116. https://doi.org/10.1016/j.egypro.2015.03.238

95. Liu S, Yu Y, Xu Z et al (2022) Efficient corncob biorefinery for ethanol initiated by a novel pretreatment of densifying lignocellulosic biomass with sulfuric acid. Fermentation 8:1–15. https://doi.org/10.3390/fermentation8110661

96. Mithra MG, Jeeva ML, Sajeev MS, Padmaja G (2018) Comparison of ethanol yield from pretreated lignocellulo-starch biomass under fed-batch SHF or SSF modes. Heliyon 4:e00885. https://doi.org/10.1016/j.heliyon.2018.e00885

97. Rojas-Chamorro JA, Romero-García JM, Cara C et al (2020) Improved ethanol production from the slurry of pretreated brewers' spent grain through different co-fermentation strategies. Bioresour Technol 296:122367. https://doi.org/10.1016/j.biortech.2019.122367

98. Sarris D, Matsakas L, Aggelis G et al (2014) Aerated vs non-aerated conversions of molasses and olive mill wastewaters blends into bioethanol by Saccharomyces cerevisiae under non-aseptic conditions. Ind Crops Prod 56:83–93. https://doi.org/10.1016/j.indcrop.2014.02.040

99. Dourou M, Economou CN, Aggeli L et al (2021) Bioconversion of pomegranate residues into biofuels and bioactive lipids. J Clean Prod 323:129193. https://doi.org/10.1016/j.jclepro.2021.129193

100. Economou CN, Aggelis G, Pavlou S, Vayenas DV (2011) Single cell oil production from rice hulls hydrolysate. Bioresour Technol 102:9737–9742. https://doi.org/10.1016/j.biortech.2011.08.025

101. Valdés G, Mendonça RT, Parra C, Aggelis G (2020) Patterns of lignocellulosic sugar assimilation and lipid production by newly isolated yeast strains from chilean valdivian forest. Appl Biochem Biotechnol 192:1124–1146. https://doi.org/10.1007/s12010-020-03398-4

102. Weerasinghe WMLI, Madusanka DAT, Manage PM (2021) Isolation and identification of cellulase producing and sugar fermenting bacteria for second-generation bioethanol production. Int J Renew Energy Dev 10:699–711. https://doi.org/10.14710/ijred.2021.35527

103. Song Z, Zhang C (2015) Anaerobic codigestion of pretreated wheat straw with cattle manure and analysis of the microbial community. Bioresour Technol 186:128–135. https://doi.org/10.1016/j.biortech.2015.03.028

Authors and Affiliations

Priyadarshani S. Sadalage[1] · Mudasir A. Dar[2] · Ana Cláudia Paiva-Santos[3,4] · Kiran D. Pawar[1]

✉ Kiran D. Pawar
kdp.snst@unishivaji.ac.in; pawarkiran1912@gmail.com

1 School of Nanoscience and Biotechnology, Shivaji University, Kolhapur, Maharashtra, India

2 Biofuel's Institute, School of the Environment and Safety Engineering, Jiangsu University, Zhenjiang 212013, China

3 Department of Pharmaceutical Technology, Faculty of Pharmacy of the University of Coimbra, University of Coimbra, Coimbra, Portugal

4 REQUIMTE/LAQV, Group of Pharmaceutical Technology, Faculty of Pharmacy of the University of Coimbra, University of Coimbra, Azinhaga de Santa Comba, 3000-548 Coimbra, Portugal